

Densification of $\text{Bi}_{0.5}\text{Na}_{0.5}\text{ZrO}_3$ ceramic using liquid-phase sintering method

Panupong Jaiban^a, Sukanda Jiansirisomboon^{a,b}, Anucha Watcharapasorn^{a,b,*}

^a Department of Physics and Materials Science, Faculty of Science, Chiang Mai University, Chiang Mai 50200, Thailand

^b Materials Science Research Centre, Faculty of Science, Chiang Mai University, Chiang Mai 50200, Thailand

*Corresponding author, e-mail: anucha@stanfordalumni.org

Received 14 Mar 2011

Accepted 31 Aug 2011

ABSTRACT: Lead-free bismuth sodium zirconate (BNZ) ceramics with formula $\text{Na}_{0.5}\text{Bi}_{0.5}\text{ZrO}_3/x\text{Bi}_2\text{O}_3$ with $x = 0, 2, 3, 4,$ and 6 wt% were prepared by liquid-phase sintering method. The specimens were sintered at 850 and 900°C . Phase identification was investigated using X-ray diffraction technique. BNZ/4 wt% Bi_2O_3 and BNZ/6 wt% Bi_2O_3 ceramics sintered at 900°C showed impurity phase of $\text{Bi}_{7.38}\text{Zr}_{0.62}\text{O}_{12.31}$ compound due to excess additive reacted with zirconium in system. Scanning electron microscopy and energy-dispersive X-ray spectroscopy were employed to study microstructure and measure chemical composition of ceramics, respectively. The results revealed creation of bismuth oxide liquid phase at BNZ grain boundaries inhibited grain growth and decreased pore size. This caused the relative densities of the modified samples to increase.

KEYWORDS: lead-free material, bismuth sodium zirconate, sintering aid, microstructure

INTRODUCTION

Sintering process is important for fabrication of ceramic materials. One of the well-known processes is liquid-phase sintering. Usually, the purpose of the mentioned method is to enhance densification rate and to decrease the fabrication temperature of a system requiring too high temperature in a conventional solid-state sintering. The microstructures of ceramics produced by liquid-phase sintering consist of two phases: (1) the crystalline grains and (2) the grain boundary phase resulting from the solidified liquid¹. Nowadays, the use of liquid-phase sintering method is increasing in ceramic components such as 96% alumina substrates for computer packages, bearing, silicon nitride extrusion dyes, etc². Moreover, it is also used in fabrication of electronic devices. Examples are actuators, sensors, transducers, etc.

Recently, $\text{Bi}_{0.5}\text{Na}_{0.5}\text{ZrO}_3$ ceramic (BNZ) was successfully fabricated^{3,4}. The novel material promotes interesting dielectric properties including the diffuse phase transition at high temperature ($T_c \approx 425^\circ\text{C}$). A material having a high Curie temperature is presumed to be a promising candidate for various electronic devices such as multilayer capacitors, detectors, MEMs, sensors, actuators etc. On the other hand, its dielectric constant at room temperature was rather low (300; 0.1 kHz) but the electrical conductivity was quite high

(9×10^{-6} S/m; 0.1 kHz). Similarly, in firing process, the green body seemed to require a high sintering temperature of 1100°C . As it does not conserve energy, it is considered too expensive.

To resolve the mentioned problem, several research attempted to apply liquid-phase method in order to enhance microstructure evolution and reduce sintering temperature of many systems i.e., bismuth sodium titanate ($\text{Bi}_{0.5}\text{Na}_{0.5}\text{TiO}_3$)⁵ and lead zirconate titanate $\text{Pb}(\text{Zr,Ti})\text{O}_3$ ^{6,7} ceramics that are well known and have been studied extensively⁸. Because it provides high Curie temperature and has possible applications, $\text{Bi}_{0.5}\text{Na}_{0.5}\text{ZrO}_3$ ceramic is considered to be interesting for our studying. Meanwhile, investigation which involves using liquid-phase sintering technique with $\text{Bi}_{0.5}\text{Na}_{0.5}\text{ZrO}_3$ ceramic has not been reported. Therefore, the aim of this work is to study densification of $\text{Bi}_{0.5}\text{Na}_{0.5}\text{ZrO}_3$ ceramic at low firing temperature ($850\text{--}900^\circ\text{C}$) by employing liquid-phase sintering process with Bi_2O_3 since it has low melting point and is known to be one of the widely used sintering aids for improvement of ceramic microstructure^{9,10}.

MATERIALS AND METHODS

The specimen was fabricated according to the formula ($\text{Bi}_{0.5}\text{Na}_{0.5}\text{ZrO}_3$)/10 wt% Na_2CO_3 . Na_2CO_3 content

was used to help complete calcination reaction¹¹. The powders were prepared by a conventional mixed-oxide method. The starting materials used in this study were ZrO₂ (99%, Riedel-de Haën), Bi₂O₃ (98%, Fluka) and Na₂CO₃ (99.5%, RdH). The mixtures of oxides were ball milled in ethanol for 24 h. The mixed powder was dried at 150 °C for 24 h and calcined in a closed alumina crucible at a temperature of 800 °C for 2 h. Then, the calcined powder was ball milled again for 6 h and was calcined again at the same temperature and time.

After obtaining BNZ powder, BNZ/*x*Bi₂O₃ mixture with *x* = 0, 2, 3, 4, and 6 wt% were prepared by ball milling for 5 h. All powders were dried at 150 °C for 24 h. After sieving, a few drops of 3 wt% PVA (polyvinyl alcohol) was added to the mixed powders as a binder before being pressed into pellets with a diameter of 10 mm using a uniaxial press with 1.0 ton weight for 15 s. Binder removal was carried out by heating the pellets to 500 °C for 1 h. These pellets were subsequently sintered at 850 and 900 °C for 2 h dwell time under its own atmosphere in a closed alumina crucible.

All samples were prepared for X-ray diffraction analysis. The sintered pellets were polished by abrasive paper and cleaned by ultrasonic technique. Phase identification of BNZ and BNZ/Bi₂O₃ ceramics were investigated using an X-ray diffractometer (XRD, Phillip Model X-pert) in a 2θ range of 20–90°. For microstructure observation, sintered samples were polished employing abrasive paper and alumina particle. After that, all of specimens were etched at 800 °C for 15 min. Scanning electron microscopy (SEM) and energy-dispersive X-ray spectroscopy were used to observe microstructure and measure chemical composition, respectively. Average sizes of grain and pore were measured using lineal analysis^{12,13}. The relative densities of all samples were calculated using their measured bulk densities determined by Archimedes' method¹⁴ (AD-1653) and their theoretical densities from simulated X-ray diffraction pattern.

RESULTS

X-ray patterns of BNZ and BNZ/Bi₂O₃ ceramics sintered at 850 and 900 °C compared with BNZ powder are shown in Fig. 1a and b, respectively. POWDER CELL software¹⁵ was used to simulate X-ray pattern resembling the pattern of BNZ powder obtained from experiment. The analysis resulting from the program revealed that the material possessed orthorhombic perovskite structure. This was in agreement with the previous report^{3,4}. The space group of BNZ was Pnma and its lattice parameters were *a* = 5.7742 Å,

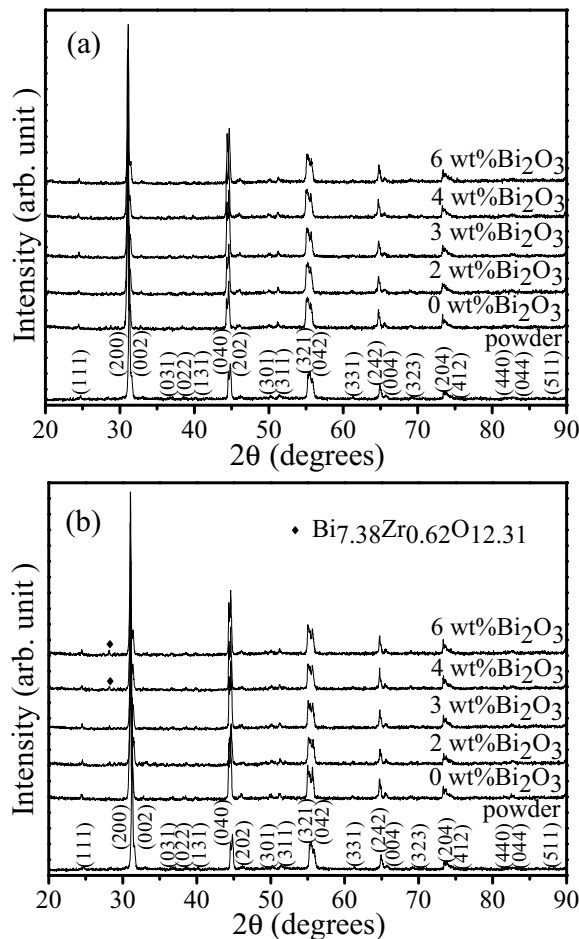


Fig. 1 X-ray diffraction patterns of BNZ powder and BNZ/Bi₂O₃ ceramics (a) sintered at 850 °C and (b) sintered at 900 °C.

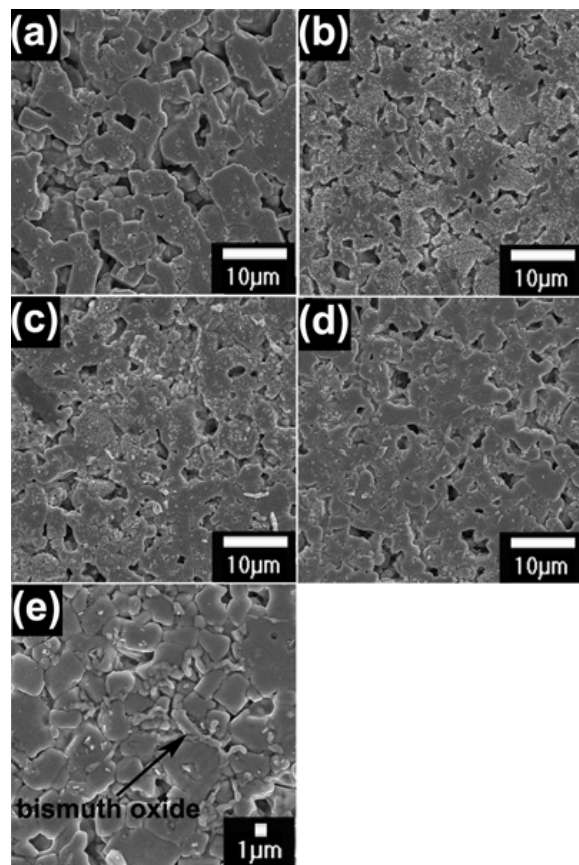
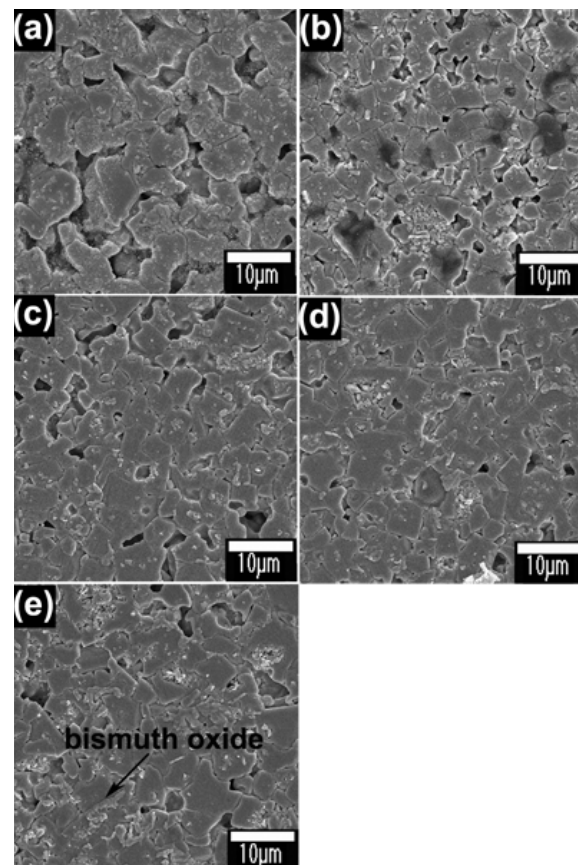
b = 8.1443 Å, and *c* = 5.7037 Å. The unit cell volume and theoretical density were 266.833 Å³ and 6.353 g/cm³, respectively. In addition, non-perovskite phase of Bi_{7.38}Zr_{0.62}O_{12.31} compound (PDF no. 43-0445) was also found with BNZ/4 wt% Bi₂O₃ and BNZ/6 wt% Bi₂O₃ materials sintered at 900 °C.

Fig. 2a–e presented SEM micrographs of BNZ and BNZ/*x*Bi₂O₃ ceramics sintered at 850 °C where *x* = 2, 3, 4, and 6 wt%, respectively. It indicated that all consisted of crystalline grains and pores having various sizes. Average grain and pore sizes are given in Table 1. Both values tended to decrease when Bi₂O₃ concentration was increased. The presence of Bi₂O₃-based liquid phase at grain boundary area of modified material could be seen apparently in BNZ system containing maximum additive content (BNZ/6 wt% Bi₂O₃).

Microstructures of BNZ/*x*Bi₂O₃ ceramics sin-

Table 1 Grain and pore size of BNZ/Bi₂O₃ ceramics sintered at different temperatures.

Ceramics	sintered at 850 °C		sintered at 900 °C	
	Grain size (μm)	Pore size (μm)	Grain size (μm)	Pore size (μm)
BNZ	4.77 ± 0.96	1.58 ± 0.94	4.81 ± 0.53	0.82 ± 0.48
BNZ/2Bi ₂ O ₃	4.69 ± 0.69	0.85 ± 0.19	3.82 ± 0.22	0.30 ± 0.21
BNZ/3Bi ₂ O ₃	3.59 ± 0.50	0.48 ± 0.28	4.09 ± 0.75	0.47 ± 0.23
BNZ/4Bi ₂ O ₃	3.52 ± 0.38	0.47 ± 0.09	3.84 ± 0.59	0.24 ± 0.11
BNZ/6Bi ₂ O ₃	3.47 ± 0.49	0.47 ± 0.20	3.58 ± 0.34	0.14 ± 0.08

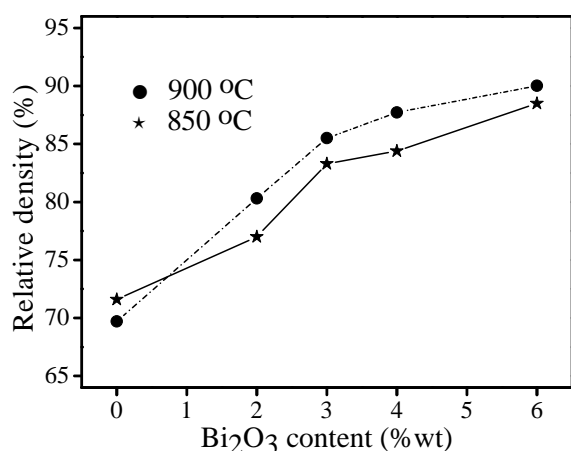
**Fig. 2** SEM micrographs of BNZ/*x*Bi₂O₃ ceramics sintered 850 °C where *x* = (a) 0, (b) 2, (c) 3, (d) 4, and (e) 6 wt%.**Fig. 3** SEM micrographs of BNZ/*x*Bi₂O₃ ceramics sintered 900 °C where *x* = (a) 0, (b) 2, (c) 3, (d) 4 and (e) 6 wt%.

tered at 900 °C where *x* = 0, 2, 3, 4, and 6 wt% are shown in Fig. 3a–e, respectively. Their SEM images showed structural features which were similar with those of ceramics sintered at 850 °C. Size of Bi_{0.5}Na_{0.5}ZrO₃ grains and pores seemed to indicate roughly decreasing trend with an increase of Bi₂O₃ concentration. Likewise in un-doped and doped BNZ systems sintered at 850 °C, amorphous liquid phase of additive was observed clearly at grain boundaries of BNZ ceramic with 6 wt% added Bi₂O₃.

Demonstration of Bi₂O₃-based liquid phase existing at BNZ/6 wt% Bi₂O₃ ceramics sintered at 850 and 900 °C was carried out using energy-dispersive X-ray spectroscopy. The chemical composition results of selected areas between crystalline grain and grain boundaries inserted by liquid phase of both specimens are given in Table 2 in unit of atomic percentage. It revealed that all areas are composed mainly of bismuth, sodium, zirconium, and oxygen elements. Nevertheless, it could be noticed that the Bi amount

Table 2 Chemical compositions of BNZ/6 wt% Bi₂O₃ sintered at different temperatures.

Elements	Sintered at 850 °C		Sintered at 900 °C	
	Grain area	Boundary area	Grain area	Boundary area
Bi	13.8 ± 2.4	36.9 ± 6.9	13.3 ± 1.5	25.8 ± 3.0
Na	9.2 ± 1.5	4.5 ± 1.3	9.0 ± 0.5	6.7 ± 2.6
Zr	15.3 ± 5.2	7.6 ± 3.8	14.8 ± 2.5	2.3 ± 2.4
O	61.6 ± 6.1	51.0 ± 9.2	63.9 ± 3.8	65.2 ± 1.7

**Fig. 4** Relative density values of BNZ and BNZ added Bi₂O₃ ceramics sintered at 850 and 900 °C.

existing at the grain boundary area of BNZ ceramic was higher than that within grain.

Fig. 4 showed the relative density values of ceramic specimens. For samples sintered at 850 °C, the maximum value was found to be 88.5% for BNZ/6 wt% Bi₂O₃. Mentioned densities were increased with increasing Bi₂O₃ content. In case of ceramics sintered at 900 °C, relative density value was maximized close to 90% with BNZ/6 wt% Bi₂O₃. This increasing trend was not different from BNZ and BNZ/Bi₂O₃ ceramics sintered at 850 °C.

DISCUSSION

According to the X-ray diffraction results of pure BNZ ceramics sintered at temperature of 850 and 900 °C, it could be seen that the patterns were in agreement with its calcined powder. Sintering process at both temperatures indicated that it could produce phase pure Bi_{0.5}Na_{0.5}ZrO₃ material and did not cause stoichiometry deviation during fabrication. In case of the Bi₂O₃-added systems sintered at 850 and 900 °C, all samples did not possess XRD diffraction pattern characteristics that were different from those of un-doped

BNZ specimens sintered at the same temperature. Also, bismuth oxide phase was not detected. It was assumed that XRD technique was not sensitive enough to confirm a presence of this additive phase in BNZ system although adding concentration was more than 5 wt%. On the other hand, a weak impurity peak of Bi_{7.38}Zr_{0.62}O_{12.31} compound existing approximately at $2\theta = 28^\circ$ was found with BNZ/*x*Bi₂O₃ ceramics sintered at 900 °C where *x* = 4 and 6 wt%. Excess Bi₂O₃ content was presumed to react with ZrO₂ in the system at high temperature to form mentioned phase. The result was similar to a study by Sood et al¹⁶, who reported that this non-perovskite phase occurred at temperature above 850 °C and increased with increasing of Bi₂O₃. Hence in samples sintered at 850 °C, this second phase was therefore not found in Bi₂O₃-doped BNZ ceramics.

With respect to the microstructural evidence of pure BNZ ceramic sintered at 850 and 900 °C, it could be seen that both materials contained large non-uniform crystalline grains in a size range of 4.77–4.81 μm and many open pores with size up to 1 μm. Creation of large BNZ grains was expected which was attributed to a rapid migration of the boundaries during final stage of conventional solid-state firing. The mentioned behaviour also led to coalescence of the pores causing the average pore size to increase. Influences of rapid grain growth and pore coalescence on microstructure evolution were found in another ceramic systems such as sintering of TiO₂¹⁷ as well as UO₂¹⁸. Minimum relative density data of un-modified samples sintered at both temperatures were correlated well with their microstructures containing large pores. On the contrary, the observed microstructures of Bi₂O₃-added BNZ ceramics less than 4 wt% Bi₂O₃ at 850 and 900 °C showed a slight decrease of BNZ grain and pore sizes to an approximate range of 3.5–4 μm and 0.2–0.5 μm, respectively. Their densities were therefore enhanced. However, SEM images could not demonstrate clearly the existence of bismuth-oxide based liquid phase at BNZ grain boundaries and this made it difficult to see effect of additive sintering aid on enhancing microstructural evolution. In case of microstructural feature of BNZ/6 wt% Bi₂O₃ fired at temperature of 850 and 900 °C, it was observed that average grain size of both cases were decreased to 3.5 μm. Doped solid particles were assumed to affect microstructural evolution of Bi_{0.5}Na_{0.5}ZrO₃ material due to the melting of additive to form liquid at temperature above 825 °C¹⁹ and provided a path for enhanced matter transport at grain boundaries. Usually, diffusion of atoms and ions through a liquid is much faster than in a solid¹. However, the distance

of diffusion path depended on the volume fraction of liquid. Increase of the volume fraction providing long diffusion distance led to decrease the rate of grain growth²⁰. From the contribution of liquid phase, size of grains of modified BNZ ceramic at maximum Bi_2O_3 concentration sintered at temperature of 850 and 900 °C were decreased up to 27% when compared with pure material fired at the same temperature. This behaviour was in agreement with several reports attempting to explain the dependence of grain growth on the volume fraction of liquid^{21–23}. In addition, the presence of Bi_2O_3 -based liquid phase and inhibition of grain growth were expected to assist filling and elimination of pore during the fabrication process. It provided a result of average pore size decreasing to less than 0.5 μm . The measured maximum relative values (89–90%) in both samples were accompanied by a decrease of size and number of pores. This seemed to agree well with a study on adding Bi_2O_3 in fabrication of $\text{Bi}_{0.5}\text{Na}_{0.5}\text{TiO}_3$ ceramic⁵. In addition, SEM micrographs indicating solidified liquid at BNZ grain boundaries and numerical details of Bi concentration between grain as well as grain boundary area could confirm clearly that mentioned material was bismuth oxide although it was not detected with XRD analysis. Non-perovskite liquid of bismuth oxide at grain boundaries built on the path for diffusion further influenced microstructural development.

Based on this study, $\text{Bi}_{0.5}\text{Na}_{0.5}\text{ZrO}_3$ ceramic implied enhancement of densification employing liquid-phase sintering process as Bi_2O_3 sintering aid at firing condition below 1100 °C. However, addition of Bi_2O_3 more than 4 wt% induced unwanted $\text{Bi}_{7.38}\text{Zr}_{0.62}\text{O}_{12.31}$ compound at sintering temperature of 900 °C. Thus the best condition found in this study was BNZ/6 wt% Bi_2O_3 sintered at 850 °C. Accordingly, sintering at temperature of 850 °C and added Bi_2O_3 content higher than 6 wt% were believed to be the main factors for obtaining the product of phase pure BNZ ceramic with relative density close to 100%. In the near future, preparation of BNZ ceramic with increased added Bi_2O_3 concentration will be investigated.

In conclusion, Bi_2O_3 -doped $\text{Bi}_{0.5}\text{Na}_{0.5}\text{ZrO}_3$ ceramics were successfully fabricated using the liquid-phase sintering method at low temperature. Bi_2O_3 material produced liquid phase at grain boundaries of $\text{Bi}_{0.5}\text{Na}_{0.5}\text{ZrO}_3$ ceramics and increased diffusion distance. This influenced the microstructural evolution of BNZ system including a reduction of grain growth rate, size of grain, number of pores and pore size. An improved change of these parameters caused densification of pure ceramic to enhance. In conse-

quence, it promoted an increase of relative density value. In firing at 900 °C, excess adding of Bi_2O_3 (> 4 wt%) induced formation of $\text{Bi}_{7.38}\text{Zr}_{0.62}\text{O}_{12.31}$ compound. The optimum sintering temperature for this material should therefore be less than 900 °C with Bi_2O_3 added as a sintering aid.

Acknowledgements: This work is financially supported by the National Metal and Materials Technology Center (MTEC), the National Science and Technology Development Agency (NSTDA), the Thailand Research Fund (TRF), and the National Research University Project under Thailand's Office of the Higher Education Commission (OHEC). The Faculty of Science and the Graduate School, Chiang Mai University is also acknowledged. We would also like to thank financial support from the Thailand Research Fund through the Royal Golden Jubilee Ph.D. program.

REFERENCES

1. Rahaman MN (1950) *Sintering of Ceramics*, Taylor & Francis group, Boca Raton.
2. Lee WE, Rainforth WM (1994) *Ceramic Microstructure Property Control by Processing*, Chapman & Hall, London, p 35.
3. Lily K, Kumari K, Prasad K, Yadav KL (2007) Dielectric and impedance study of lead-free ceramic: $(\text{Na}_{0.5}\text{Bi}_{0.5})\text{ZrO}_3$. *J Mater Sci* **42**, 4652–9.
4. Prasad K, Lily K, Kumari K, Yadav KL (2007) Hopping type of conduction in $(\text{Na}_{0.5}\text{Bi}_{0.5})\text{ZrO}_3$ ceramic. *J Phys Chem Solid* **68**, 1508–14.
5. Wang XX, Tang XG, Kwok KW, Chan HLW, Choy CL (2005) Effect of excess Bi_2O_3 on electrical properties and microstructure of $(\text{Bi}_{1/2}\text{Na}_{1/2})\text{TiO}_3$ ceramics. *Appl Phys Mater Sci Process* **80**, 1071–5.
6. Nielsen ER, Ringgaard E, Kosec M (2002) Liquid-phase sintering of PZT using PbO-WO_3 additive. *J Eur Ceram Soc* **22**, 1847–55.
7. Corker DL, Whatmore RW, Ringgaard E, Wolny WW (2000) Liquid-phase sintering of PZT ceramics. *J Eur Ceram Soc* **20**, 2039–45.
8. Rödel J, Klaus WJ, Seifert TP, Anton EM, Granzow T (2009) Perspective on the development of lead-free piezoceramics. *J Am Ceram Soc* **92**, 1153–77.
9. Chung HH, Yang CF, Chen KH, Diao CC (2009) The influences of excess Bi_2O_3 content on the characteristics of $0.8(\text{Bi}_{0.5}\text{K}_{0.5})\text{TiO}_3-0.2\text{BaTiO}_3$ ceramics. *Ferroelectrics* **385**, 89–96.
10. Tay KW, Fu YP, Huang QF, Jang FH (2010) Effect of Bi_2O_3 additives on sintering and microwave dielectric behavior of $\text{La}(\text{Mg}_{0.5}\text{Ti}_{0.5})\text{O}_3$ ceramics. *Ceram Int* **38**, 1239–44.
11. Jaiban P, Jiansirisomboon S, Watcharapasorn A (2010) Synthesis of lead-free $\text{Bi}_{0.5}\text{Na}_{0.5}\text{ZrO}_3$ powder. *J Met Mater Miner* **20**, 141–4.

12. Underwood EE (1970) *Quantitative stereology*, Addison-Wesley, Reading.
13. Fulrath RM, Pask JA (1968) *Ceramic Microstructures*, Wiley, New York.
14. German RM (1946) *Sintering Theory and Practice*, John Wiley & Sons, New York, p 26.
15. Kraus W, Nolze G (1996) Powder Cell – a program for the representation and manipulation of crystal structures and calculation of the resulting X-ray powder patterns. *J Appl Crystallogr* **29**, 301–3.
16. Sood K, Singh K, Pandey OP (2010) Synthesis and characterization of Bi-doped zirconia for solid electrolyte. *Ionics* **16**, 549–54.
17. Yan MF (1981) Microstructural control in the processing of electronic ceramics. *Mater Sci Eng* **48**, 53–72.
18. Kingery WD, Francis B (1965) Grain growth in porous compacts. *J Am Ceram Soc* **48**, 546–7.
19. Liu C, Lan Z, Jiang X, Yu Z, Sun K, Li L, Liu P (2008) Effect of sintering temperature and Bi₂O₃ content on microstructure and magnetic properties of LiZn ferrites. *J Magn Magn Mater* **320**, 1335–9.
20. Kang TK, Yoon DN (1978) Coarsening of tungsten grains in liquid nickel-tungsten matrix. *Metall Mater Trans* **9**, 433–8.
21. German RM (1985) *Liquid Phase Sintering*, Plenum Press, New York.
22. Vorhees PW (1992) Ostward ripening of two-phase mixtures. *Annu Rev Mater Sci* **22**, 197–215.
23. Yang SC, Manni SS, German RM (1990) The effect of contiguity on growth kinetics in liquid-phase sintering. *J Met* **42**, 16–9.